Journal of Electroceramics 3:4, 387–397, 1999

Phase Transformation and Temperature Dependence of Relative Permittivity for A-site Substituted $Sr(Y_{0.5}Ta_{0.5})O_3$ Perovskites

T. FUJII, J. TAKAHASHI & S. SHIMADA

Division of Materials Science and Engineering, Graduate School of Engineering, Hokkaido University, Kita-13 Nishi-8 Kita-ku, Sapporo 060-8628, Japan

K. KAGEYAMA

Sumitomo Metal Ind., Ltd., 1, Higashi Mukaijima-Nishinomachi, Amagasaki 660-0856, Japan

Submitted December 23, 1998; Revised April 1, 1999; Accepted May 4, 1999

Abstract. A-site cation substitution with Ba^{2+} or Ca^{2+} ions was made for the ordered complex perovskite $Sr(Y_{0.5}Ta_{0.5})O_3$ to correlate the structure evolution and the change in the temperature coefficient of relative permittivity ($TC\varepsilon_r$) with the cation substitution. The crystal symmetry of the solid solutions at room temperature changed as monoclinic → rhombohedral → cubic with the corresponding A-site cation species of $Ca^{2+} \rightarrow Sr^{2+} \rightarrow Ba^{2+}$. On heating, the rhombohedral phase of $Sr(Y_{0.5}Ta_{0.5})O_3$ was firstly transformed to the cubic phase with a lower symmetry ($F\bar{4}3m$ or F432) at 1000°C and further to the ideal cubic phase (Fm3m) at 1300°C. The similar phase transformation behavior at elevated temperatures was observed for each of the Ba^{2+}-substituted perovskites, both the phase transformation temperatures being lowered with increasing Ba^{2+} content. ε_r of the ordered perovskites monotonously increased over the temperature range where the phase transformation regions from monoclinic to rhombohedral or from rhombohedral to cubic ($F\bar{4}3m$ or F432) occurred. On the other hand, a subtle symmetry change in the cubic phase from $F\bar{4}3m$ (F432) to Fm3m caused a remarkable change in the $TC\varepsilon_r$ from positive to negative at the transformation temperature. These results suggested that the positive $TC\varepsilon_r$ is essentially correlated to the relaxation of the tilting of the BO_6 octahedra in the perovskite structure on heating.

Keywords: complex perovskites, strontium yttrium tantalum oxide, cation substitution, phase transformation, temperature coefficient of relative permittivity

1. Introduction

The complex perovskites, $A(B'B'')O_3$, can be readily synthesized by variable cation combinations for A-, B′-, and B″-sites. Hence, many physical properties can be controlled by the cation combinations. Since some of the complex perovskites had been found to have excellent microwave dielectric properties [1,2], investigations on the formation and dielectric properties of various complex perovskites have been conducted to develop dielectric components suitable for microwave applications [3,4]. The present authors found that $Sr(Ga_{0.5}Ta_{0.5})O_3$ (hereafter referred to as SGT) is a B-site disordered perovskite with excellent microwave properties ($\varepsilon_r = 27$, $Qf = 91500$ GHz, $\tau_f = -50$ ppm/K) [4]. Additionally, the substitution of the A-site Sr^{2+} with Ba^{2+} and Ca^{2+} was made for the SGT perovskite, and changes were described in the crystal structure and dielectric properties with the A-site cation substitution [5]. While Ba^{2+} cations could be incorporated in the A-site sublattice up to 55 mol% without cation ordering, the A-site Sr^{2+} ions were completely replaced by the Ca^{2+} ions. The crystal symmetry of the Ca^{2+}-substituted $(Sr_{1-y}Ca_y)(Ga_{0.5}Ta_{0.5})O_3$ perovskites correspondingly changed from cubic ($0 \leq y \leq 0.5$) to orthorhombic ($0.8 \leq y \leq 1$) with increasing Ca^{2+} content. A substantial lowering in microwave Q-value observed for the solid solutions containing $10 \sim 20$ mol% Ba^{2+} or Ca^{2+} ions might be explained

by the lack of structural long-range ordering. The temperature coefficient of relative permittivity ($TC\varepsilon_r$) measured at 1 MHz considerably changed in a specific composition range between SGT (120 ppm/K) and $(Sr_{0.9}Ba_{0.1})(Ga_{0.5}Ta_{0.5})O_3$ (20 ppm/K). Structural considerations suggested that the $TC\varepsilon_r$ change might be correlated with the linkage of BO_6 octahedra in the perovskite structure.

Among the dielectric properties, the $TC\varepsilon_r$ is a very important intrinsic property because most practical dielectric components must have a temperature independent characteristic under operating environments. Nonetheless, little information is available concerning factors dominating the $TC\varepsilon_r$ change in dielectrics [6,7]. In the present study, in order to obtain useful information on the relationship between the structural change associated with BO_6 octahedra in the perovskite and the $TC\varepsilon_r$, the authors selected a B-site cation ordered perovskite, $Sr(Y_{0.5}Ta_{0.5})O_3$ (SYT), as the main composition and conducted a serial A-site cation substitution with Ba^{2+} or Ca^{2+} for SYT. It is known that the A-site Sr^{2+} ions can be completely replaced by the Ba^{2+} (BYT) or Ca^{2+} (CYT) ions and the crystal systems of SYT, BYT, and CYT are rhombohedral [8], cubic [9], and monoclinic [10], respectively. Besides, it was reported that the crystal system of SYT was transformed from rhombohedral to cubic at 640°C [8]. However, there have been no reports on the change of crystal system, phase transformation behavior, and dielectric properties of the solid solutions in the SYT-BYT-CYT system. Therefore, in this paper, the solid solutions $(Sr_{1-x}Ba_x)(Y_{0.5}Ta_{0.5})O_3$ and $(Sr_{1-y}Ca_y)(Y_{0.5}Ta_{0.5})O_3$ were synthesized, and their crystal system and phase transformation were studied by the Rietveld method using high temperature X-ray powder diffraction data. Additionally, the $TC\varepsilon_r$ was examined in detail to relate the structural evolution with the A-site cation substitution.

2. Experimental Procedure

The powder samples for sintering were prepared using the conventional solid state reaction. Highly purified powders of carbonates ($SrCO_3$, $BaCO_3$, $CaCO_3$) and oxides (Y_2O_3, Ta_2O_5) were weighed and ball-milled with distilled water for 24 h in a plastic container. After drying, the mixed powders were calcined at 1300°C for 6 h in air. The calcined powders were pressed into disks (12 mm diameter and 3 mm thickness) under uniaxial (50 MPa) and cold isostatic (100 MPa) pressing. The green compacts were sintered in the temperature range 1550∼1750°C for 24 h in air. High temperature X-ray powder diffractometry (HT-XRD: JEOL JDX-3500) was conducted under conditions as follows; radiation: CuKα, temperature range: 25∼1300°C, heating rate: 10°C/min, heating duration at a fixed temperature prior to measurement: 30 min, measured 2θ range: 15∼100° with step scan. The HT-XRD data were analyzed by the Rietveld method (program RIETAN97) [11] to determine the lattice parameters and crystal systems. Dielectric properties at 1 MHz were measured with a digital LCR meter (YHP-4285 A) for Ag-coated samples using the 3-probe method in a temperature range from −150 to 600°C.

3. Results and Discussion

3.1. Crystal Structures of the Solid Solutions

Since no report describing the XRD data of SYT is available, those for SYT sintered at 1600°C for 24 h are given in Table 1. Structural data of SYT can be seen in Table 2 with those of BYT formed in this study. At first, solid solutions between SYT and BYT were synthesized to examine structural change with Ba^{2+} substitution. Figure 1 (A) shows the XRD patterns of some selected samples of the Ba^{2+}-substituted solid solutions $(Sr_{1-x}Ba_x)(Y_{0.5}Ta_{0.5})O_3$ sintered at 1600°C for 24 h. Single phase ordered perovskites were obtained for all the Ba^{2+}-substituted samples. The crystal systems of the solid solutions were rhombohedral (R3m) and cubic ($F\bar{4}3m$ or F432), for the samples with $0 \leq x \leq 0.4$ and $0.5 \leq x \leq 0.9$, respectively.

Table 3 indicates the XRD data for CYT sintered at 1550°C for 24 h. CYT has a lower structural symmetry (monoclinic) with an appearance of many XRD peaks so that weak peaks with relative intensity less than 1% are not included in Table 3. Lattice parameters are also given in Table 2 with other structural data. For the Ca^{2+}-substituted solid solutions $(Sr_{1-y}Ca_y)(Y_{0.5}Ta_{0.5})O_3$, a similar structural analysis was performed. Figure 1 (B) shows the XRD patterns of some selected samples sintered at 1550°C for 24 h. The crystal system of the Ca^{2+}-substituted solid solutions was changed from rhombohedral

Table 1. X-ray diffraction data of $Sr(Y_{0.5}Ta_{0.5})O_3$ sintered at 1600°C for 24 h

2θ/°	d/nm	I(obs)	I(cal)	hkl
18.51	0.4789	4	4	111
18.63	0.4760	12	10	−111
21.51	0.4129	21	19	200
24.13	0.3686	2	2	−210
30.53	0.2926	100	100	220
30.67	0.2913	99	99	−220
32.37	0.2764	1	1	221
35.94	0.2497	2	2	311
36.06	0.2489	4	5	3–11
36.12	0.2484	2	2	−311
39.40	0.2285	<1	<1	−320
40.84	0.2208	<1	<1	−3–21
43.82	0.2064	59	64	400
45.04	0.2012	<1	<1	322
45.19	0.2005	2	2	410
47.80	0.1901	1	1	331
47.95	0.1896	1	1	−3–31
48.10	0.1890	2	2	−331
49.22	0.1850	4	4	420
49.41	0.1843	4	4	−420
50.45	0.1807	2	2	421
54.17	0.1692	23	20	422
54.43	0.1684	44	39	4–22
54.52	0.1682	22	19	−422
57.70	0.1596	<1	<1	333
57.87	0.1592	1	1	511
58.00	0.1589	1	1	5–11
58.09	0.1587	1	1	−333

(R3m: $0 \leq y \leq 0.2$) to monoclinic (P2/m: $0.4 \leq y \leq 1$). Since the R_I factor of the solid solution with $y = 0.3$ was found to be large ($R_I = 12\%$) by the Rietveld analysis, the crystal system could not determined to be either rhombohedral or monoclinic.

A very weak peak of Y_2O_3 (marked ▲ in Fig. 1 (B)) was observed in each sample with the composition range $0 < y \leq 0.6$. The synthesis of single phase Ca^{2+}-substituted perovskites was attempted in the composition range $0 < y \leq 0.6$. Solid solutions with fixed Ca^{2+} contents were fabricated by sintering at a higher temperature (1700°C) or using a powder prepared via the columbite method in which preformed $YTaO_4$ was mixed with $SrCO_3$ and $CaCO_3$ stoichiometrically. Alternatively, the Y_2O_3 content in a starting powder was lowered by 0.5 or 1.0 mol% relative to stoichiometry. Despite these attempts, no single phase perovskite was synthesized for the samples examined. These results suggested that the B-site Y^{3+} deficient perovskite might be thermodynamically stabilized in this compositional range. Figure 2 shows changes in the lattice parameters and cell

Table 2. Structural data of SYT, BYT and CYT

	$Sr(Y_{0.5}Ta_{0.5})O_3$	$Ba(Y_{0.5}Ta_{0.5})O_3$	$Ca(Y_{0.5}Ta_{0.5})O_3$
Crystal system	Rhombohedral	Cubic	Monoclinic
Space group	R3m	Fm3m	P2/m
Lattice parameter	$a = 825.7$ pm	$a = 844.3$ pm	$a = 806.7$ pm
			$b = 806.0$ pm
			$c = 806.7$ pm
	$\alpha = 89.74°$		$\beta = 92.18°$

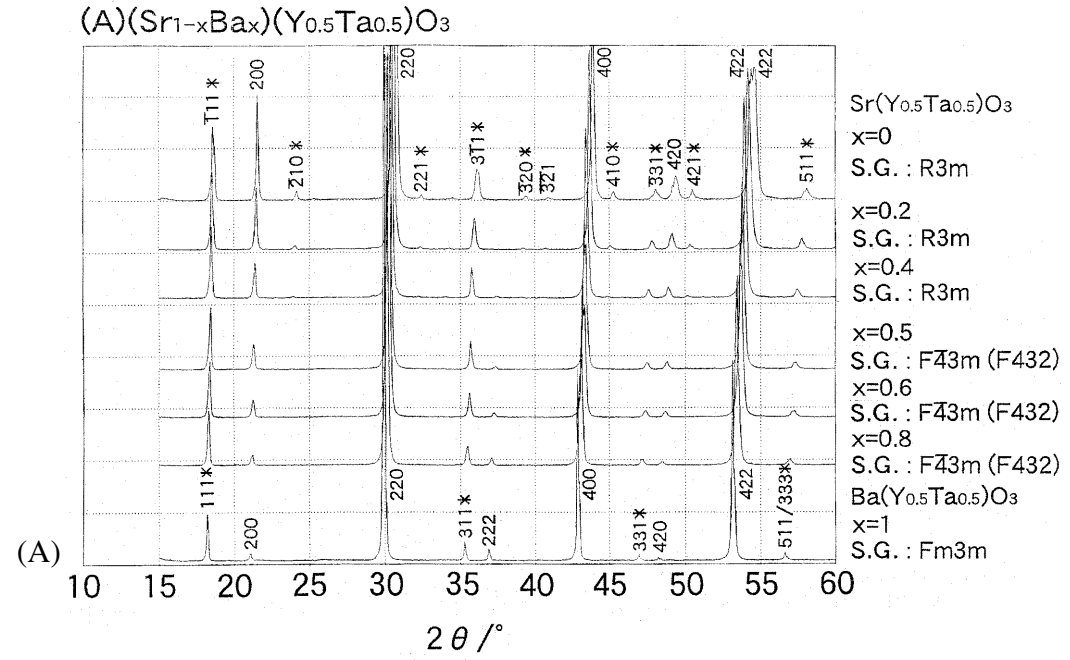

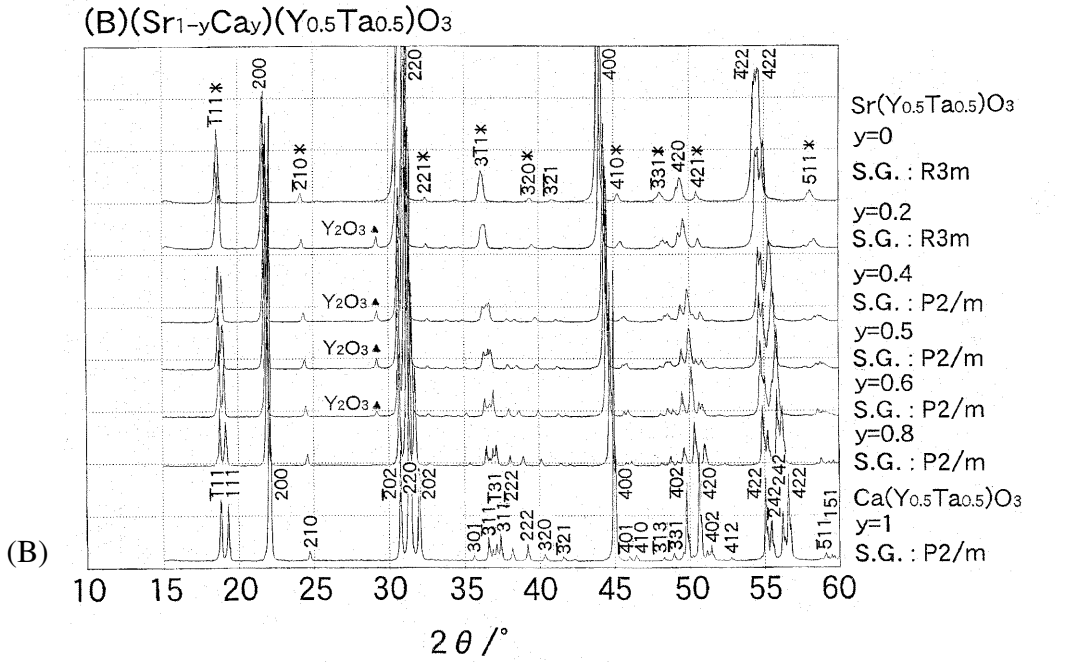

Fig. 1. X-ray diffraction patterns of some selected samples of (A) Ba^{2+}-substituted and (B) Ca^{2+}-substituted solid solutions.

Table 3. X-ray diffraction data of $Ca(Y_{0.5}Ta_{0.5})O_3$ sintered at 1550°C for 24 h

2θ/°	d/nm	I(obs)	I(cal)	hkl
18.81	0.4714	13	10	− 111
19.30	0.4596	12	10	111
22.04	0.4031	62	58	200
22.04	0.4031	62	58	020
24.68	0.3605	1	1	210
30.74	0.2906	27	29	− 202
31.36	0.2850	100	100	220
31.97	0.2797	24	25	202
35.59	0.2521	1	1	301
36.56	0.2456	6	4	− 311
36.83	0.2439	3	2	− 131
37.09	0.2422	3	2	131
37.35	0.2406	6	4	311
38.15	0.2357	3	2	− 222
39.27	0.2298	3	2	222
40.31	0.2236	1	1	320
41.54	0.2172	1	1	− 321
44.94	0.2015	43	39	400
44.95	0.2015	21	19	040
45.96	0.1973	1	1	− 401
46.41	0.1955	1	1	410
48.28	0.1884	1	1	− 313
48.92	0.1860	3	2	− 331
49.55	0.1838	3	2	331
49.77	0.1831	9	7	− 402
50.17	0.1817	1	1	313
50.60	0.1802	16	13	420
50.60	0.1802	16	13	240
51.13	0.1785	1	1	− 412
51.42	0.1776	7	5	402
52.74	0.1734	1	1	412
55.05	0.1667	25	22	− 422
55.45	0.1656	13	11	− 242
56.22	0.1635	12	10	242
56.59	0.1625	23	20	422
59.08	0.1562	1	1	− 511
59.46	0.1553	1	1	− 151
59.64	0.1549	1	1	151
60.00	0.1541	1	1	511

volume with A-site cation content over the whole composition range.

3.2. *Phase Transformation of the Solid Solutions*

The phase transformation temperature of SYT from rhombohedral to cubic, which was reported to be 640°C [8], was first reconfirmed by HT-XRD analysis. Because the HT-XRD data measured at around 640°C showed that no phase transformation occurred in the temperature range, data at higher temperatures were successively collected for SYT. Figure 3 shows the change in the HT-XRD patterns of SYT with increasing temperatures ((A): 900°C, (B): 1000°C, (C): 1300°C). The HT-XRD patterns of (A) and (B) in Fig. 3 are apparently similar. The Rietveld analysis revealed that the crystal structure of SYT at 900°C was rhombohedral (R3m: $a = 833.3$ pm, $\alpha = 89.94°$). However, it was not able to refine the lattice parameters of the sample measured at 1000°C as rhombohedral because of the divergence of the parameter α. It could be analyzed to be cubic phase with space group of $F\bar{4}3m$ or F432. Figure 4 indicates changes in the lattice parameter of SYT with

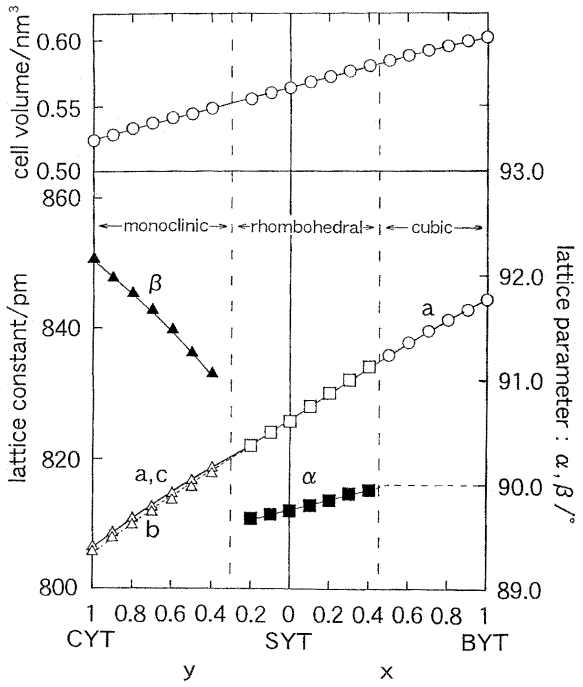

Fig. 2. Changes in lattice parameters and cell volume of the solid solutions at room temperature.

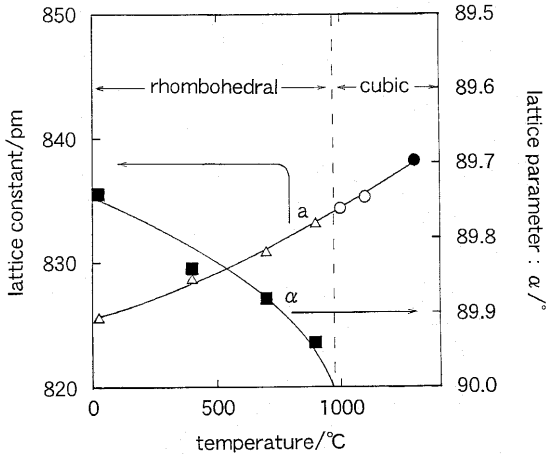

Fig. 4. Changes in the lattice parameters of the $Sr(Y_{0.5}Ta_{0.5})O_3$ with heating.

increasing temperature. On heating the SYT sample, α approached from 89.74° at room temperature to 90° at 1000°C, and the crystal structure changed from rhombohedral to cubic. Thus the phase transformation temperature was determined to be 1000°C.

Comparing the HT-XRD patterns of Fig. 3 (B) and 3 (C), the peaks at 1000°C were broadened at the higher 2θ region. In order to explain this difference in

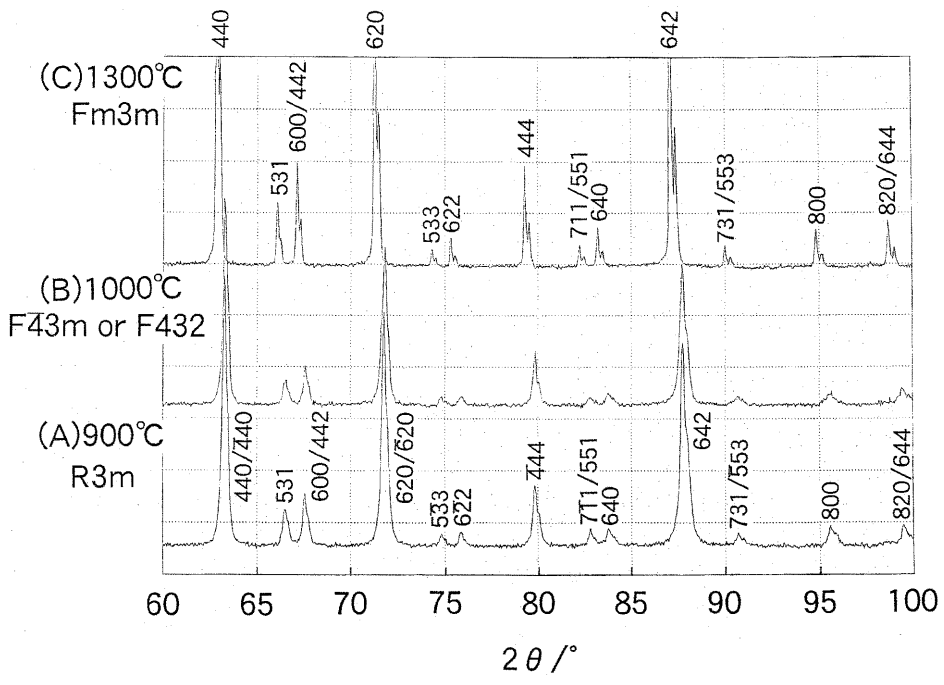

Fig. 3. HT-XRD patterns of the $Sr(Y_{0.5}Ta_{0.5})O_3$ heated at (A) 900°C, (B) 1000°C, and (C) 1300°C.

the peak shapes, the crystal structure was refined in detail in the temperature range 1000∼1300°C. The R_I factor of the Rietveld analysis was calculated for the sample at 1000°C using space group of Fm3m, F$\bar{4}$3m, or F432. It was estimated to be 4.0%, 2.9%, and 3.1% for each space group, respectively. This analysis implied that the XRD data could be best fitted to the subtle distorted structure (F$\bar{4}$3m or F432) rather than the ideal (1:1) type ordered structure (Fm3m). Unfortunately, it was not able to determine the space group of either F$\bar{4}$3m or F432 because of few appreciable differences in the R_I factors. As for the sample at 1300°C, however, F$\bar{4}$3m (F432) was not appropriate for its space group due to the resulting negative thermal vibration parameter. Hence, it was clear that the SYT perovskite has the Fm3m structure at 1300°C.

The phase transformation temperature for each of the Ba^{2+} or Ca^{2+}-substituted solid solutions was determined by a similar analysis (Table 4 shows the R_I factors of some selected samples). Thus the results of the crystal structure change with increasing temperature for the SYT-BYT-CYT system can be seen in Fig. 5. For the Ba^{2+}-substituted solid solutions, shown at the right of Fig. 5, the rhombohedral phase of the samples with $0 \leq x \leq 0.4$ (marked with △) was transformed to the cubic phase (F$\bar{4}$3m or F432) above each temperature (T_{RC}) shown by a broken line. The T_{RC} decreased with increasing Ba^{2+} content; i.e., 1000° (SYT) → 700°C ($x = 0.2$)→200°C ($x = 0.4$). The temperature at which the transformation from F$\bar{4}$3m (F432) to Fm3m within the cubic structure was completed is also included in Fig. 5 (marked with ●). Similarly, the phase transformation behavior of the Ca^{2+}-substituted perovskites can be seen at the left of Fig. 5. Each of the rhombohedral phase ($0 < y \leq 0.2$)

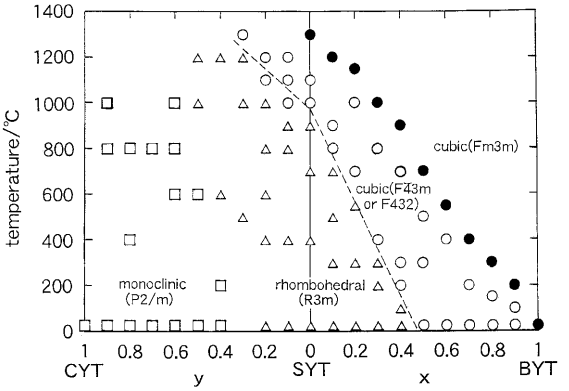

Fig. 5. A diagram showing phase transformations for the CYT-SYT-BYT system.

was transformed to the cubic phase (F$\bar{4}$3m or F432) at a higher temperature than for the Ba^{2+}-substituted solid solutions. The monoclinic phase (□) of the samples with $0.4 \leq y \leq 1$ would also be transformed to the rhombohedral phase (△) at elevated temperatures (T_{MR}). However, it was difficult to determine precisely the T_{MR} because the large R_I values ($R_I = 15\%$) were obtained for the samples heated in wide temperature ranges (e.g., 200∼600°C and 600∼1000°C for samples with $y = 0.4$ and $y = 0.5$, respectively).

In summary, the crystal system of the solid solutions in the SYT-BYT-CYT system was evolved with changes in the A-site cation ($Ca^{2+} \rightarrow Sr^{2+} \rightarrow Ba^{2+}$) and also with increasing temperature. The corresponding transformation sequence is as follows: monoclinic (P2/m)→rhombohedral (R3m)→cubic (F$\bar{4}$3m or F432) and finally idealized cubic (Fm3m).

Table 4. RI factors of some selected samples calculated for different space groups

		Ri/% Space group		
Composition	Temperature/°C	Fm3m	F$\bar{4}$3m	F432
$X = 0$ (SYT)	1000	4.0	2.9	3.1
$X = 0.2$	700	4.9	4.3	4.2
$X = 0.5$	25	3.7	3.3	3.2
	500	5.0	4.3	4.3
$X = 0.8$	25	3.4	3.0	2.8
$Y = 0.2$	1200	4.5	3.5	3.6

3.3. Change in $TC\varepsilon_r$ during Phase Transformation

According to the phase transformation behavior shown in Fig. 5, the temperature dependence of ε_r of each perovskite sample for which a phase transformation occurred in the temperature range of $-150 \sim 600°C$ was measured at 1 MHz. The results are given in Fig. 6. For the Ba^{2+}-substituted samples with $x = 0.3$ (marked with ○ in Fig. 6) and $x = 0.4$ (△) whose phase transformation region are indicated in Fig. 6, the corresponding ε_r monotonously increases over each T_{RC} region ($TC\varepsilon_r = 130$ ppm/K). As for the Ca^{2+}-substituted sample with $y = 0.4$ (●) in which the transformation from monoclinic to rhombohedral was expected to occur at $200 \sim 600°C$, no appreciable change in ε_r was observed within the temperature region ($TC\varepsilon_r = 100$ ppm/K). On the contrary, those with the compositions of $x = 0.6$ (■ in Fig. 6 (A)), 0.8 (● in Fig. 6 (B)), 0.9 (▲ in Fig. 6 (B)), and 1.0 (■ in Fig. 6 (B)) clearly had a distinctive maximum in the ε_r value ($\varepsilon_{r(\max)}$) at each specified temperature. The $\varepsilon_{r(\max)}$ temperature decreased with increasing Ba^{2+} content such as $530°C \rightarrow 270°C \rightarrow 140°C \rightarrow -15°C$ for the corresponding composition described above. As can be seen from Fig. 4, these temperatures definitely coincided with those above which each perovskite compound has the idealized Fm3m structure. Obviously, the transition from a positive $TC\varepsilon_r$ to a negative one was closely related to the phase transformation in the cubic region from $F\bar{4}3m$ (F432) to Fm3m but not associated with either phase transformation from monoclinic to rhombohedral and rhombohedral to slightly distorted cubic.

Some investigations were conducted on the $TC\varepsilon_r$ changes of various complex perovskites in relation to the linkage manner of the BO_6 octahedra in the perovskite structure [12–14]. Colla et al. [12] studied the structure–$TC\varepsilon_r$ relationship for $(Ba_{1-x}Sr_x)(Zn_{0.33}Nb_{0.67})O_3$ solid solutions (BSZN). Based on a structural phase diagram obtained for the BSZN system, they tried to quantitatively correlate the changes in the temperature coefficient of capacitance (τ_c) with the appearance and types of the BO_6 octahedra tilting. In their discussion using an expression proposed by Bosman and Havinga [6], it could be deduced that in the highly symmetric cubic structure the strength of the dipoles are constrained to become smaller with the increasing thermal energy (i.e., negative τ_c), whereas this effect can be strongly inhibited in the tilted and distorted structure (positive τ_c). Similarly, the present authors had examined the $TC\varepsilon_r$ change of $Sr(Ga_{0.5}Ta_{0.5})O_3$ with A-site cation substitution on the basis of the following equation derived by Bosman and Havinga [6]

$$\begin{aligned}\frac{1}{(\varepsilon-1)(\varepsilon+2)}\left(\frac{\partial\varepsilon}{\partial T}\right)_P &= -\frac{1}{3V}\left(\frac{\partial V}{\partial T}\right)_P \\ &\quad + \left[\frac{V}{\alpha_m}\left(\frac{\partial\alpha_m}{\partial V}\right)_T \times \frac{1}{3V}\left(\frac{\partial V}{\partial T}\right)_P\right] \\ &\quad + \frac{1}{3\alpha_m}\left(\frac{\partial\alpha_m}{\partial T}\right)_V \\ &= A + B + C\end{aligned}$$

where α_m is the polarizability of a macroscopic, small sphere with a volume V and the third term (C) is the only term that depends directly on the structures and their symmetries. A possible explanation for a large change in the $TC\varepsilon_r$ observed with the Ba^{2+}-substituted sample was that a structurally subtle change in the BO_6 octahedra tilting might substantially alter the temperature dependence of the polarizability (the term C in the above equation) [5]. This consideration fundamentally coincided with that given by Colla et al. [14].

In order to explain the result obtained in the present complex perovskites, a similar consideration based on the tilting of the BO_6 octahedra was applied. The idealized structure of Fm3m consists of the BO_6 octahedra linked in a straightforward manner to each other. If a little distortion due to the displacement of some cations is introduced in the idealized structure, then it causes a subtle tilting of the BO_6 octahedra linkage and hence the structure might be transformed to the $F\bar{4}3m$ (F432) structure. When the crystal symmetry becomes much lower such as rhombohedral and monoclinic, the tilting of the BO_6 octahedra linkage is progressively increased [15,16]. Therefore, it is reasonably considered that the change in the $TC\varepsilon_r$ might be substantially affected by the occurrence of the tilting of the BO_6 octahedra, but not by the degree of it. Fundamentally, the $TC\varepsilon_r$ of a dielectric predominantly reflects the temperature dependence of polarizability (TCα) in a structural unit. For a material consisting of an ideal structural unit without any distortion, the TCα becomes negative [6,7]. If some distortion was introduced in the structure, e.g., the tilting of the BO_6 octahedra in the perovskite structure, the distortion can be gradually softened with increasing temperature, which might lead to a positive TCα. Thus the $TC\varepsilon_r$ change from positive to negative

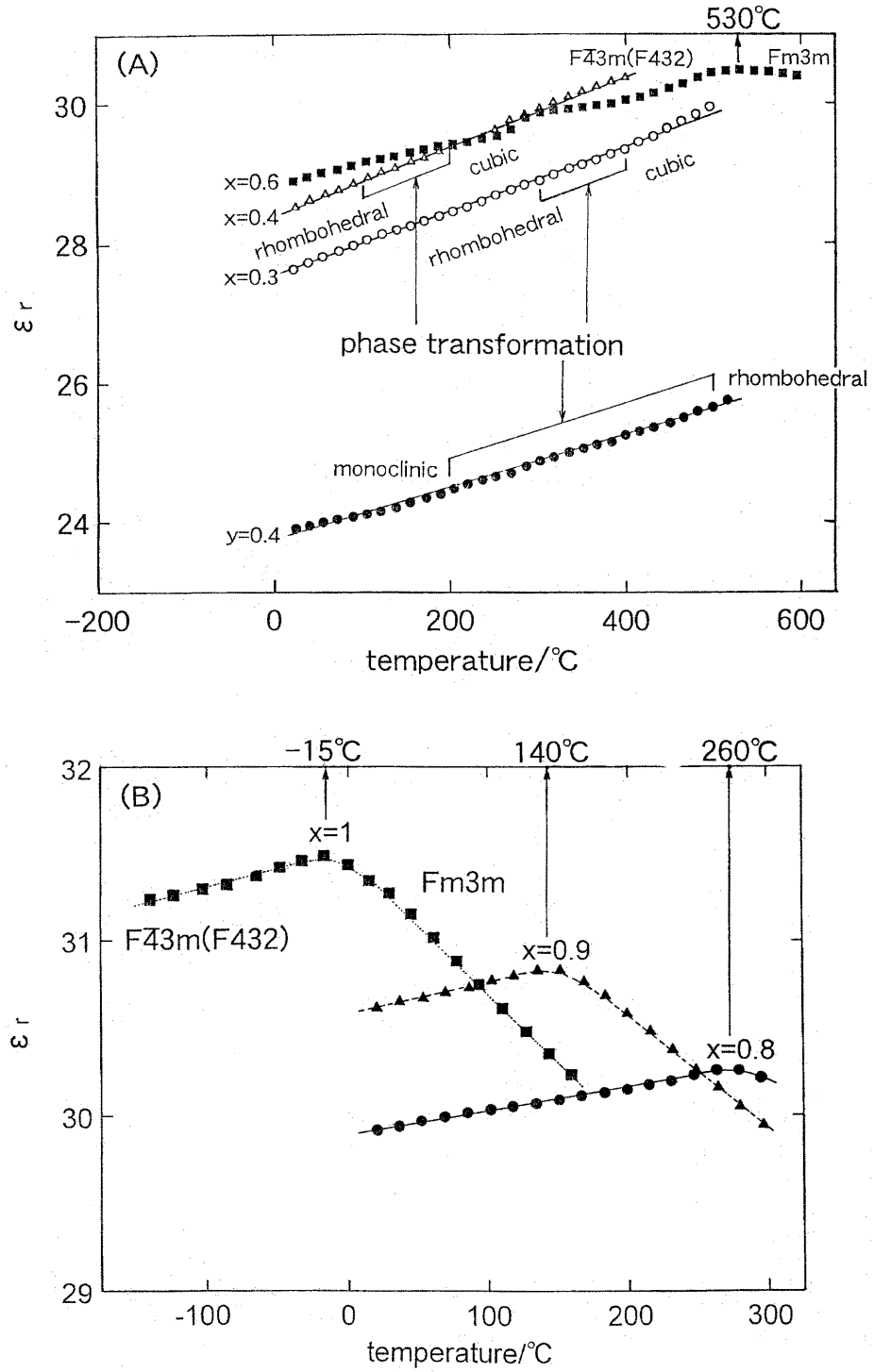

Fig. 6. Temperature dependence of relative permittivity for some selected samples measured at 1 MHz.

with increasing temperature observed in the Ba^{2+}-substituted perovskites might be qualitatively explained by the release of structural distortion during the phase transformation from $F\bar{4}3m$ (F432) to Fm3m.

Figure 7 shows the dielectric properties of the solid solutions examined. Broken lines correspond to the compositional range $0 < y \leq 0.6$ where a small amount of Y_2O_3 coexisted. ε_r was gradually increased by changing the A-site cation $Ca^{2+} \rightarrow Sr^{2+} \rightarrow Ba^{2+}$; $\varepsilon_r = 22$ (CYT)$\rightarrow$24 (SYT)$\rightarrow$31 (BYT). Such an increase in ε_r with the A-site cation species ($Ca^{2+} \rightarrow Sr^{2+} \rightarrow Ba^{2+}$) was observed in many other complex perovskites. Compared with the disordered solid solutions $(Sr_{1-x}Ba_x)(Ga_{0.5}Ta_{0.5})O_3$ and $(Sr_{1-y}Ca_y)(Ga_{0.5}Ta_{0.5})O_3$ previously studied by the present authors [5], a tendency for ε_r to increase with changing A-site cations ($Ca^{2+} \rightarrow Sr^{2+} \rightarrow Ba^{2+}$) was similar to that of the present study, but only a small change was observed for the $Sr(Ga_{0.5}Ta_{0.5})O_3$-based solid solutions (A = Ca: $\varepsilon_r = 25 \rightarrow$ A = Sr: $\varepsilon_r = 27 \rightarrow$ A = $Sr_{0.5}Ba_{0.5}$: $\varepsilon_r = 28.5$) [5]. Probably, the occurrence of the B-site cation ordering might be responsible for the enhanced $TC\varepsilon_r$ change in the present perovskites.

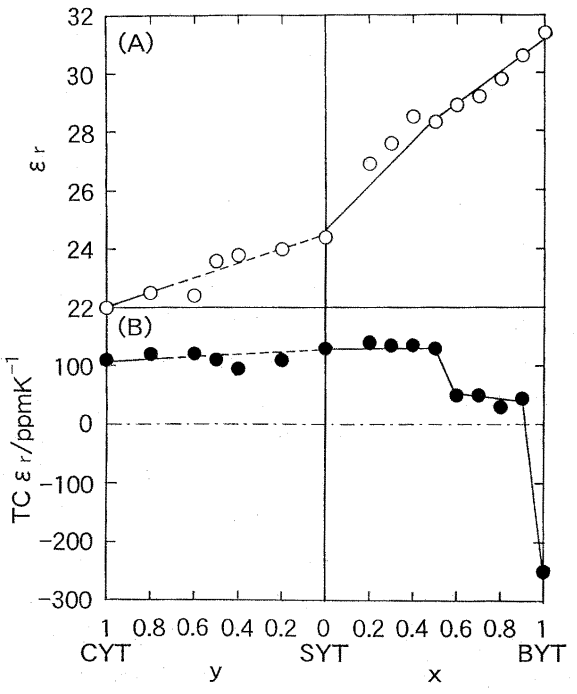

Fig. 7. Changes in (A) relative permittivity and (B) $TC\epsilon_r$ (measured at 25∼150°C) with A-site cation species.

The $TC\varepsilon_r$s of the solid solutions calculated from changes in ε_r at 25∼150°C are plotted against varying A-site cation content in Fig. 7 (B). The $TC\varepsilon_r$ of each sample with $0 \leq y \leq 1$ and $0 \leq x \leq 0.5$ was nearly constant (100∼130 ppm/K), although the crystal system was changed depending on the A-site cation species (monoclinic$\rightarrow$rhombohedral$\rightarrow$cubic). As for the samples with $0.6 \leq x \leq 0.9$ which already had the cubic symmetry with only a slight distortion, smaller $TC\varepsilon_r$s were obtained (30∼50 ppm/K). At the extreme composition of BYT, the $TC\varepsilon_r$ was abruptly reduced to -250 ppm/K. This negative value was ascribed to the reverse temperature dependence after the maximum ε_r (Fig. 6 (A)).

4. Conclusions

In the present study, crystal structure, phase transformation, and dielectric properties were studied for the ordered complex perovskites $(Sr_{1-x}Ba_x)(Y_{0.5}Ta_{0.5})O_3$ and $(Sr_{1-y}Ca_y)(Y_{0.5}Ta_{0.5})O_3$, and changes in the temperature coefficient of relative permittivity was correlated to the structure evolution during heating. The results were as follows:

1. The A-site Sr^{2+} ions were completely replaced by Ba^{2+} or Ca^{2+} ions. The crystal systems of the Ba^{2+}-substituted solid solutions at room temperature were rhombohedral (R3m; $0 \leq x \leq 0.4$), a slightly distorted cubic ($F\bar{4}3m$ or F432; $0.5 \leq x \leq 0.9$), and ideal cubic (Fm3m; $x = 1$). On the other hand, the crystal system of the Ca^{2+}-substituted solid solutions changed from rhombohedral (R3m; $0 \leq y \leq 0.2$) to monoclinic (P2/m; $0.4 \leq y \leq 1$).
2. The rhombohedral phase of the Ba^{2+}-substituted solid solutions ($0 \leq x \leq 0.4$) were transformed from the rhombohedral phase to the cubic phase ($F\bar{4}3m$ or F432) at elevated temperature. The phase transformation temperature was estimated to be 1000°C for SYT, and decreased with increasing Ba^{2+} content. On further heating, change in the space group from $F\bar{4}3m$ (F432) to Fm3m was observed for the Ba^{2+}-substituted solid solutions ($0 \leq x \leq 0.9$). Similarly, the phase transformations during heating from rhombohedral to cubic and from monoclinic to rhombohedral were observed for the Ca^{2+}-substituted solid solutions with $0 \leq y \leq 0.2$ and $0.4 \leq y \leq 0.5$, respectively.

3. ε_r of the ordered perovskites in the present system monotonously increased over the temperature range where the phase transformation from monoclinic to rhombohedral or from rhombohedral to cubic ($F\bar{4}3m$ or F432) took place. On the other hand, a subtle symmetry change in the cubic phase from $F\bar{4}3m$ (F432) to Fm3m caused a large change in the $TC\varepsilon_r$ from positive to negative at the transformation temperature. The negative $TC\varepsilon_r$ with increasing temperature might be caused by an essential characteristic in the perovskite structure consisting of ideally linked BO_6 octahedra, whereas the positive $TC\varepsilon_r$ observed for those having some structural distortion might be due to the resulting release of the distortion during heating.

References

1. S. Kawashima, M. Nishida, I. Ueda, and H. Ouchi, *J. Am. Ceram. Soc*., **66**, 421–423 (1983).
2. S. Nomura, K. Toyama, and K. Kaneta, *Jpn. J. Appl. Phys*., **21**, 624–626 (1982).
3. M. Takata and K. Kageyama, *J. Am. Ceram. Soc*., **72**, 1955–1959 (1989).
4. J. Takahashi, K. Kageyama, T. Fujii, T. Yamada, and K. Kodaira, *J. Mater. Sci: Elect*., **8**, 79–84 (1997).
5. T. Fujii, J. Takahashi, S. Shimada, and K. Kageyama, *J. Ceram. Soc. Japan*, **106**, 669–675 (1998) (in Japanese).
6. A.J. Bosman and E.E. Havinga, *Phys. Rev*., **129**, 1593–1600 (1963).
7. A.G. Cockbain and P.J. Harrop, *Brit. J. Appl. Phys. Ser. 2*, **1**, 1109–1115 (1968).
8. M.F. Kupriyanov and V.S. Filip'ev, *Sov. Phys. Cryst*., **8**, 278–283 (1963).
9. F.S. Galasso, G.K. Layden, and D.E. Flinchbaugh, *J. Chem. Phys*., **44**, 2703–2707 (1966).
10. V.S. Filip'ev and E.G. Fesenco, *Sov. Phys. Cryst*., **10**, 243–247 (1965).
11. F. Izumi, *The Rietveld Method*, ed. by R.A. Young (Oxford University Press, Oxford, 1993), pp. 236–253.
12. E.L. Colla, I.M. Reaney, and N. Setter, *J. Appl. Phys*., **74**, 3414–3425 (1993).
13. I.M. Reaney, E.L. Colla, and N. Setter, *Jpn. J. Appl. Phys*., **33**, 3984–3990 (1994).
14. E.L. Colla, N. David, C. Rau, and N. Setter, *Ferroelectrics*, **184**, 151–160 (1996).
15. A.M. Glazer, *Acta Cryst*., **B28**, 3384–3392 (1972).
16. A.M. Glazer, *Acta Cryst*., **A31**, 756–762 (1975).